ASSIGNMENT 2: 1D TRANSIENT HEAT CONDUCTION PROBLEM (GROUND).

Computational Methods in Heat and Mass Transfer

Submitted by-

Srijan Dasgupta

NOVEMBER 25, 2022

UNIVERSITAT POLITECNICA DE CATALUNYA (UPC)

Barcelona, Spain.

Problem Specification:

In this analysis, we have to examine the temporal evolution of the ground temperature distribution (Fig. 1) for a time-dependent heat conduction equation. This heat conduction equation will be assumed to be a valid model for the ground temperature (thus, we are neglecting the humidity changes or other aspects

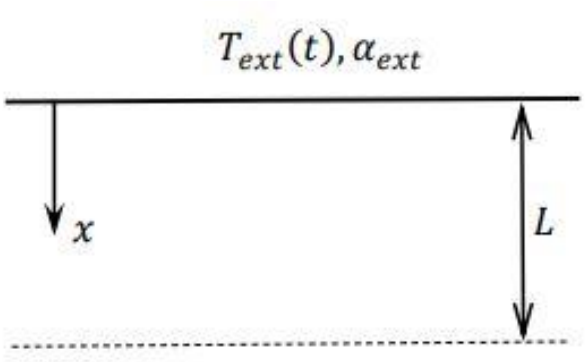

Figure 1: Schematic representation of the proposed problem.

that may actually be relevant). We have assumed a constant thermal conductivity; thus, the governing equation can be written as,

$$\rho c_p \left(\frac{dT}{dt}\right) = \lambda \left(\frac{\partial^2 T}{\partial x^2}\right)$$

The surface in contact with the outdoor ambient will be at x=0. The ground at some depth x=L (L=2m), maintains its temperature at $T=T_w$. the heat transfer coefficient α_{ext} can be considered constant, but the temperature of the medium, T_{ext}, changes by the following law:

$$T_{ext}(t) = A_0 + A_1 \sin(\omega_1 t) + A_2 \sin(\omega_2 t)$$

Where, time is in seconds, and,

$$\omega_1 = \frac{2\pi}{24 \times 3600}; \qquad \omega_2 = \frac{2\pi}{365 \times 24 \times 3600}$$

The initial temperature of the gound, t=0, is T_0.

The physical parameters chosen for the analysis are given below:

Physical Data	
L (m)	2.0
ρ (kg/m^3)	2300
c_p (J/kgK)	700
λ (W/mK)	1.6
α_{ext} (W/m^{2}K)	8.5
T_0 (^{o}C)	19.0
A_0 (^{o}C)	19.0
A_1 (^{o}C)	5.7
A_2 (^{o}C)	9.1
T_w (^{o}C)	19.0

Table 1: Physical parameters.

Methodology:

Since, the x direction is defining the width of the ground, if we change the orientation of the ground to make it horizontal instead of vertical, we can see that this problem is analogous to a rectangular plate heat conduction problem, where the left boundary is in contact with the air of varying temperature T_{ext} and a specific value of heat transfer coefficient α_{ext}, while the right boundary is kept at a constant temperature T_w.

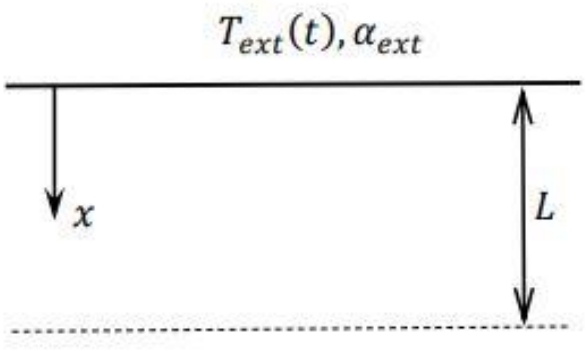

Figure 2: Ground characteristics.

For our case, the width of the ground is L, however the length and depth are not specified. Thus, we assume that this case has unit length and depth, which results in solving the problem in per unit area system.

We need to use proper indexing for the convenience of the code writing during the numerical solution. For that purpose, a small discretization has been demonstrated to explain how the discretization takes place. Here, the node which is being analyzed is called the P node and the index for this node is [i]. The left node of the analysis node is called the W node with index of [i-1], whole the right node of the analysis node is called the E node with index of [i+1]. Similarly, the left face of the of analysis node P is called 'w' face and the right face is called the 'e' face.

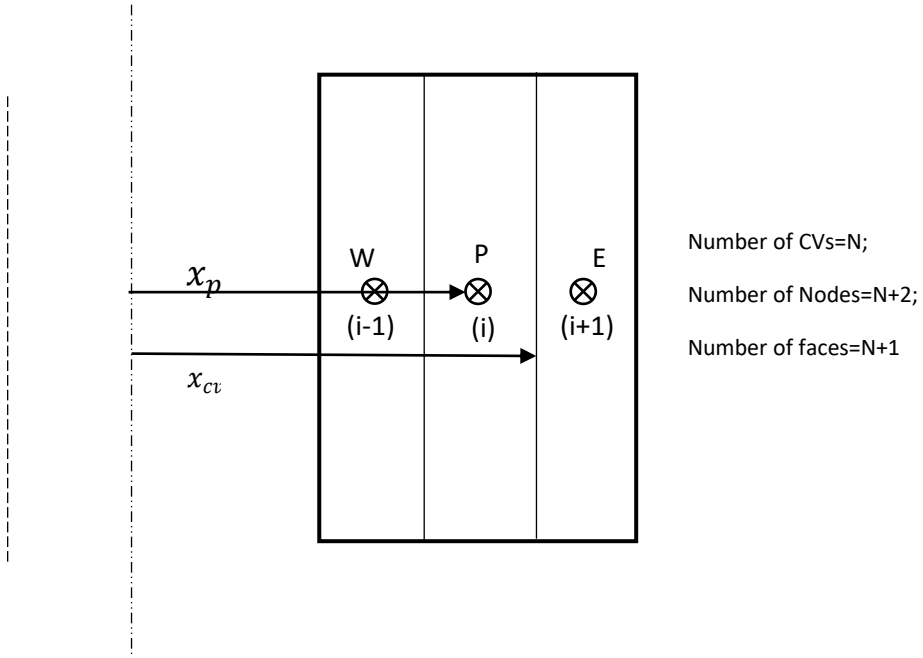

Figure 3: Ground characteristics.

As we create the control volumes of equal thickness, each of the nodes are established in the middle of each control volumes. However, we have two extra nodes at the boundary of the cylinder walls. For this particular reason, for N number of control volume discretization, we have N+2 number of nodes, where N number of nodes are central nodes, and two nodes are boundary nodes.

For the analysis itself, the position of each node and the faces were recorded with proper indexing. The example of the indexing pattern has been shown in Figure 3. Notice that the indexing is 1D since the nodal distribution is only one dimensional due to the pattern of the problem.

For the central nodes (i=2 to N+1):

Taking into consideration of the control volume with P node like Figure 3, we applied energy balance,

$$\frac{\partial}{\partial t}\oint u_p \rho dV = \dot{Q_w} - \dot{Q_e} = -\left[\lambda \frac{dT}{dx}\right]_w + \left[\lambda \frac{dT}{dx}\right]_e$$

Assuming density is constant, we can write,

$$\rho_p V_p \int_{t^n}^{t^{n+1}} \frac{\partial \bar{u}_p}{\partial t} dt = \int_{t^n}^{t^{n+1}} \sum \dot{Q}_p dt \ldots\ldots\ldots (1)$$

$$where, \sum \dot{Q}_p = \dot{Q_w} - \dot{Q_e}$$

For solid materials, the left-hand side term can be expanded as,

$$\rho_p V_p \int_{t^n}^{t^{n+1}} \frac{\partial \bar{u}_p}{\partial t} dt = \rho_p V_p \frac{({\bar{u}_p}^{n+1} - {\bar{u}_p}^{n})}{\Delta t} = \rho_p V_p \overline{C_{p_p}} \frac{({T_p}^{n+1} - {T_p}^{n})}{\Delta t}$$

Similarly, the right-hand side term can be expanded as,

$$\int_{t^n}^{t^{n+1}} \sum \dot{Q}_p dt = \left[\ \beta \sum {\dot{Q}_p}^{n+1} + (1-\beta) \sum {\dot{Q}_p}^{n}\right]$$

This value of β depends on the time integration method we want to use for solving the problem. The values of β can be expressed like the following,

$$\beta = \begin{cases} 0 & explicit \\ 1 & implicit \\ \frac{1}{2} & Crank - Nickolson \end{cases}$$

Equation (1) can be written as,

$$\rho_p V_p \overline{C_{p_p}} \frac{({T_p}^{n+1} - {T_p}^{n})}{\Delta t} = \beta \left[-\frac{\lambda_w (T_P - T_W)}{d_{PW}} + \frac{\lambda_e (T_E - T_E)}{d_{PE}}\right]^{n+1} + (1-\beta) \sum {\dot{Q}_p}^{n}$$

Where, Vp is the volume of the control volume where the node P resides. Manipulating the equation above, we can achieve the following equation for the control volumes which are the central nodes surrounded by other nodes at each direction.

$$a_P {T_P}^{n+1} = a_E {T_E}^{n+1} + a_W {T_W}^{n+1} + b_P$$

Where,

$$a_E = \frac{\beta {\lambda_e}^{n+1} S_e}{d_{PE}}$$

$$a_w = \frac{\beta {\lambda_w}^{n+1} S_w}{d_{PW}}$$

$$a_p = a_E + a_w + \frac{\rho_p V_p \overline{C_{p_p}}}{\Delta t}$$

$$b_p = \frac{\rho_p V_p \overline{C_{p_p}}}{\Delta t} {T_p}^n + (1-\beta) \sum {\dot{Q}_p}^n$$

Here, ap, ae, aw, bp are all discretization coefficients.

For node i=1:

For the left boundary node, the energy balance must be done by considering the convection between the surrounding fluid at the boundary and the heat conduction at the boundary. The left-most node adjacent to a fluid changes its temperature according to the following equation,

$$T_{ext}(t) = A_0 + A_1 \sin(\omega_1 t) + A_2 \sin(\omega_2 t)$$

Considering the value of the air temperature variation, the energy balance of the first node will be like the following,

$${\dot{Q}_{conv}}^{n+1} = {\dot{Q}_{cond}}^{n+1}$$

$$-\frac{{\lambda_e}^{n+1}\left({T_E}^{n+1} - {T_P}^{n+1}\right)}{d_{PE}} = {\alpha_A}^{n+1}({T_{ext}}^{n+1} - {T_P}^{n+1})$$

Which will result in the following equation,

$$a_P {T_P}^{n+1} = a_E {T_E}^{n+1} + b_P$$

$$a_P[1] T^{n+1}[1] = a_E[1] T^{n+1}[2] + b_P[1]$$

Where,

$$a_E = \frac{{\lambda_e}^{n+1}}{d_{PE}}$$

$$a_p = a_E + a_w + \frac{\rho_p V_p \overline{C_{p_p}}}{\Delta t}$$

$$b_p = \alpha^{n+1} {T_{ext}}^{n+1}$$

Notice that unlike the previous equation for the central nodes, the left-most node does not have any Tw term inside the equation. The absence of the term Tw is justified since for the left-most node, there is no neighbor node on the left. Similarly, for the right-most node, ae will be zero as well.

For node i=N+2:

In our case, the right most node temperature is kept at a fixed temperature T_w, thus we can say that that wall is an isothermal wall.

In that case, we can write,

$$T_P{}^{n+1} = T_w$$

$$a_p T_P{}^{n+1} = b_p$$

Where,

$$a_p = 1$$

$$b_p = T_w$$

Now that we know the relationships between the discretization coefficients and temperatures of each node, we can use a solver to solve the set of equations.

Code structure:

Steps to solve the set of equations:

1. **Input data**: We had two sets of input data: Physical data and Numerical data. Physical data included L, ρ, C_p, λ, A_0, A_1 etc. and numerical data included Ncv, δ etc.
2. **Previous calculation and vector definition**: We discretized the domain by calculating r_{cv}, r_p, V_p and then we defined matrices for the discretization coefficients.
3. **Initial temperature (t=0)**: In this stage, we defined the temperature at t=0 as current step temperature T_n.
4. **Calculation of $t^{n+1}=t^n+\Delta t$:**
   4.1. For our method, we needed to know the temperature of the next timestep as well. For this reason, we needed to estimate temperature at the next instant. A good approximation is to assume that the next timestep value is equal to the current timestep value, thus $T^{n+1*}=T^n$.
   4.2. Then, we estimated and calculated λ^{n+1}, a_e, a_w, a_p, b_p etc. using te estimated temperature value. However, for our case, the value of thermal conductivity was constant, thus the calculation was much simpler.
   4.3. In this step, we solved the discretization equations for each node.
   4.4. After solving the discretization equations, we checked whether absolute value of (T^{n+1}-T^{n+1*}) was less than tolerance or not. If the value was less than the tolerance value, we proceeded to the next step. But if the tolerance was still less than the error between the estimated value and the calculated value, we set $T^{n+1*}=T^{n+1}$ and repeated the iteration from step 4.2.
5. **New time step:** In this step, we checked whether we have more timestep or not. For the next timestep calculation we set $T^n=T^{n+1}$ and repeated the process from step 4.
6. **Final calculation and print results:** In this step, using the data generated from the code, we calculated and plotted several relevant results to explain the problem and visualize the impact of the parameters.
7. **End.**

Numerical studies:

After defining the code according to the algorithm, which was mentioned previously, we picked a set of numerical parameters on our own to get a reference solution. This reference solution will later be used to run mesh studies, time step studies, influence of physical parameters etc.

Reference case:

For our reference case, the following data were used,

Start time=0 sec

End time =100×24×3600 sec

Time step = 10000 sec

Number of control volumes = 101

Tolerance= $1e^{-09}$

Maximum number of iterations =$1e^{06}$

β=1 (Implicit method)

For this reference case, we used implicit method so that we can use a large timestep. The reason for using a large timestep for our case is to make the code faster. Since it took a significant amount of time to see the change in temperature of the air, we had to take bigger timestep to visualize the temporal evolution quickly by reducing the amount of calculation.

Thermal Behavior:

According to our problem, the initial air, ground and boundary at x=L are at same temperature. The boundary at x=L is an isothermal boundary, and the ground has no internal heat generation, thus the thermal variation of the ground will occur due to the change of air temperature at x=0.

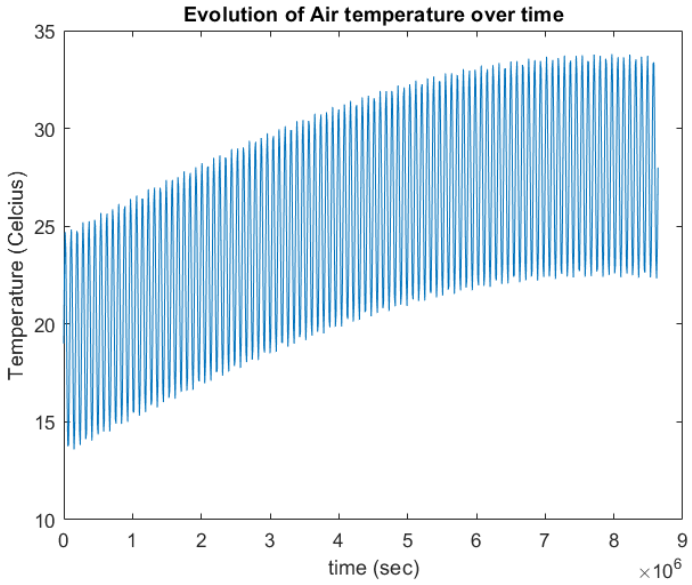

Figure 2: Thermal evolution of air with time.

Here, figure 4 illustrates the variation of the air temperature with time. It is noticeable that the variation of temperature is really small compared to time and it is an increasingly oscillatory thermal behavior.

For this reference case value, all the temperature profile for each node was stored accordingly.

Almost similar kind of trend was noticed when we plotted the temporal evolution of the ground at x=0 in figure 5, which is adjacent to the air with varying temperature. This is obvious since the ground at x=0 is at direct contact with the air.

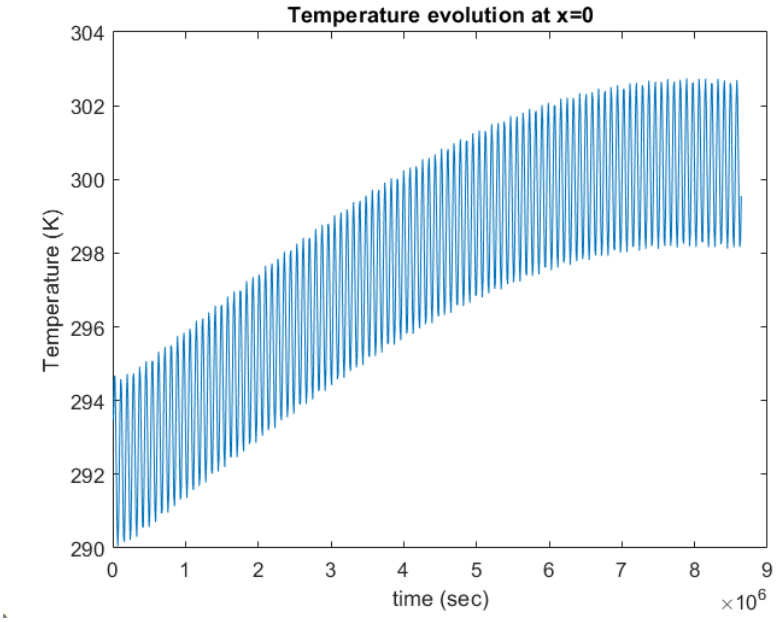

Figure 3: Temporal evolution of ground at x=0.

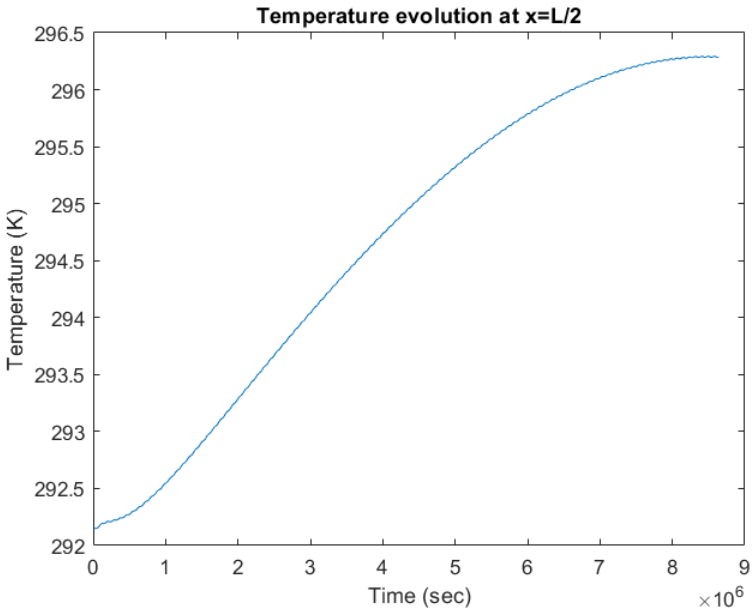

Figure 4: Temporal evolution of ground at x=L/2.

We also tried to track the temperature of the ground at x=L/2, and we noticed the trend showed in figure 6. The temperature evolution shows that the temperature of the ground at x=L/2 gradually increases with

time. Although it looks like a smooth curve, but if the curve is zoomed at an extent, it can be noticed that the temperature profile is also oscillating, but the amplitude is much less compared to the ground temperature oscillation at x=0.

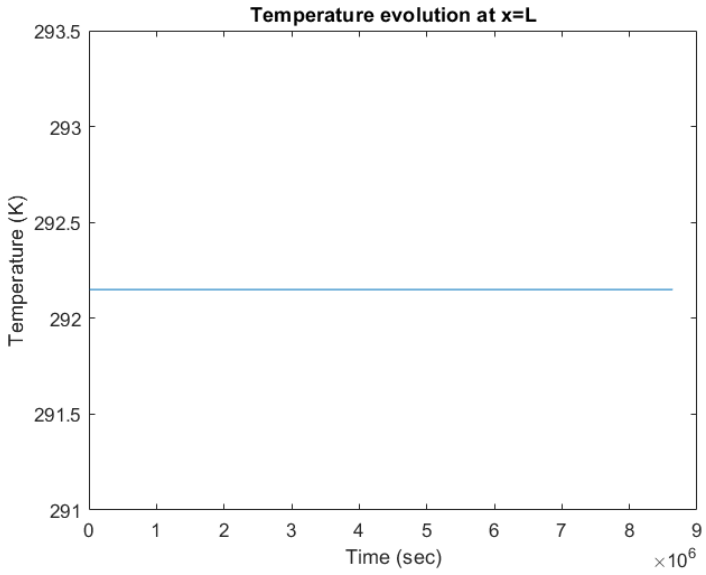

Figure 5: Temporal evolution of ground at x=L.

The temperature evolution of ground at x=L however does not change with time as we can see in figure 7. This is obvious in our case since the temperature at x=L was set to a constant temperature.

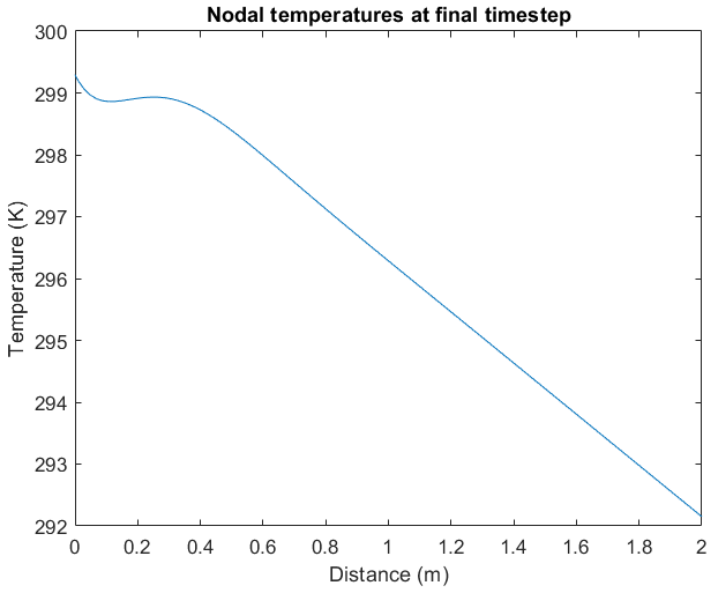

Figure 6: Temporal evolution of the ground.

Finally, we plotted the temporal evolution of the ground for all nodes at t=100×24×3600 seconds, which in our case was the final time for the unsteady case analysis. We can notice that the temperature at the right boundary is constant at 19ºC. Although the initial condition for all the nodes and the air was set to 19ºC, since the temperature of the air varied with time and the average temperature of the air increased as well, the temperature of the ground temperature increased as well. However, the temperature of the

ground was highest at the left boundary and slowly decreased as it moved to the right, since the right boundary is in an isothermal condition at 19°C.

During the evolution of the temperature of the ground, we noticed that the temperature of the ground increases very slowly, and the propagation of temperature is slow as well. Also, when the temperature of the air goes down, the ground temperature does not fall immediately. This can be explained using the physical properties which were used to study this case.

For our particular case, the thermal conductivity λ had a really small value while the specific heat C_p had a relatively large value, thus the propagation of heat was slow in the ground, and it required a large amount of heat to change the temperature of the ground to a significant scale.

Validation strategies:

There were several ways to validate the results. But for our case, we chose to use energy balance to validate our results. Also, we performed some parametric studies to verify whether our code can produce results that follow basic physical principles.

For the energy balance, we needed to see the boundary conditions of our control volume. In our case, the ground at x=0 was in contact with the air, and an isothermal wall at x=L. Thus, energy balance equation will be as following,

$$Q_{accumulation} - Q_{left} - Q_{right} = 0$$

$$\sum_{i=2}^{i=N+1} \rho_p V_p \overline{C_{p_p}} \frac{({T_p}^{n+1} - {T_p}^{n})}{\Delta t} - {\alpha_A}^{n+1} S_P \left({T_{ext}}^{n+1} - T[1]^{n+1}\right) + \frac{{\lambda_e}^{n+1} S_P (T[N+1]^{n+1} - T[N+2]^{n+1})}{d_{PE}} = 0$$

However, over the time, the value of the air temperature varies quite a lot. For this reason, the average temperatures were considered in the right side of the equation.

Using the above equation, between t=0 second and t=100×24×3600 seconds, the value of the energy balance was 0.0017.

Similarly, between the last two timesteps, the value of the energy balance was $-1.8475\times10^{-6.}$

Mesh and time discretization studies:

For understanding the mesh studies, we had to consider both time and space discretization studies. For the space discretization study, we changed the number of control volumes and evaluated the energy balance for all cases.

Table 3: Variation of mesh sizes.

Number of CVs	Timestep	Global time Energy Balance	Local time Energy balance
101 (reference)	10000	0.0017	-1.8475×10^{-6}
50	10000	0.0017	-2.8416×10^{-7}
1000	10000	0.0017	-1.0498×10^{-4}

We increased and decreased the number of CVs for the domain discretization mesh studies. We noticed that the global time energy balance for t=0 seconds to t=100×24×3600 seconds stays comparatively same for all cases. There was slight increase with increasing the number of control volumes However, when we

did the energy balance between the last two time-instances, the global energy balance value changed noticeably in comparison to each other. It also increased with increased number of control volumes.

The reason is the inherent discretization error of the global energy balance.

Later, we also did change the timesteps to study the time discretization and compared the change in the energy balance value for each case as well.

Table 4: Variation of timestep.

Number of CVs	Timestep	Global time Energy Balance
101	10000 (reference)	0.0017
101	1000	1.7260×10^{-4}
101	40000	0.0071

It was noticed that when the timestep was smaller, we had smaller error in the global energy balance and if the timestep was larger, we had larger error.

Parametric studies:

For the parametric study, we changed the parameters like geometry sizes and material properties.

Geometry sizes:

Instead of using L=2m as per the reference case, we used L=5m and L=0.5m. We noticed that the temperature increment at x=L/2 is decreased when the size is increased and the vice versa.

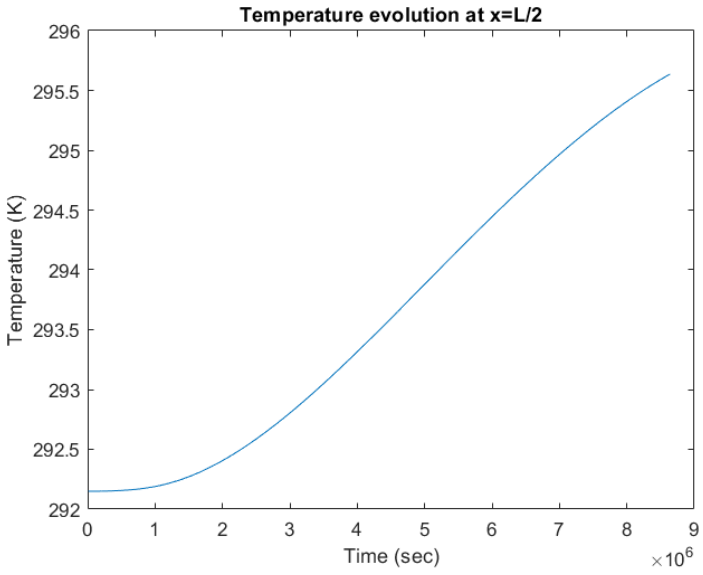

Figure 7: Temperature at x=L/2 for L=5m.

However, when decreased the thickness of the ground more and more, we noticed that the energy propagation is more prominent. The influence of the changing temperature of the boundary condition i.e., air, can be noticed significantly at x=L/2 when the value of L is really small, as seen in figure 10.

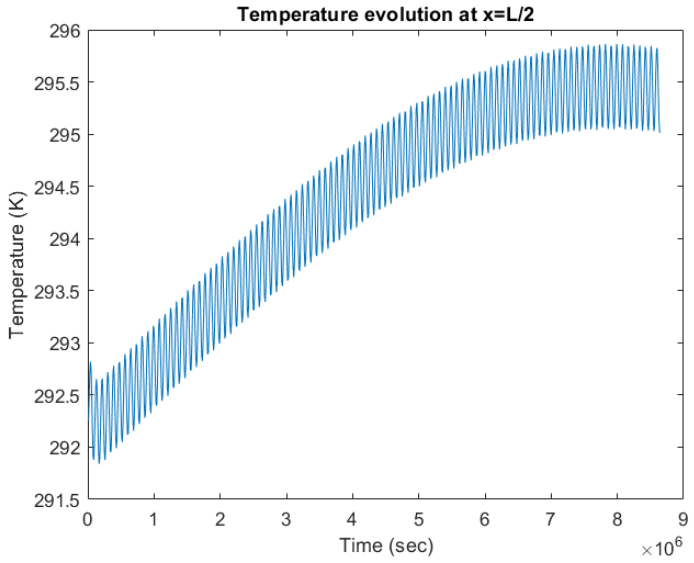

Figure 8: Temperature at x=L/2 for L=0.5m.

Thermophysical properties:

In our case, the ground material had really low thermal conductivity, but high density and specific heat values. For this particular reason, the temporal evolution is relatively slower and it takes more time and energy to increase the temperature of the ground.

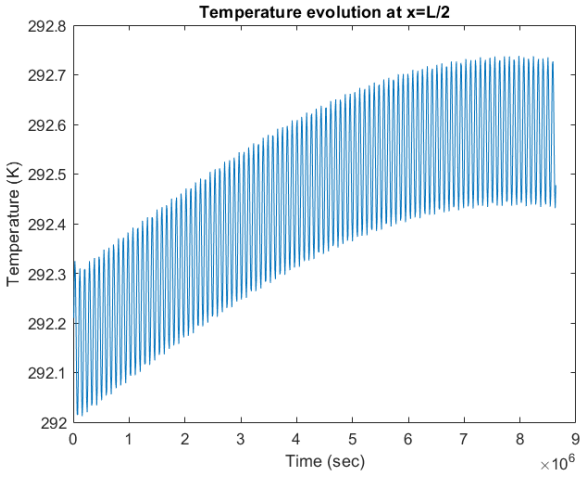

Figure 9: Temperature evolution at x=L/2 for $\lambda=1.6\times10^2$ W/mK.

However, later on, we increased the thermal conductivity, and we noticed that the temperature change at x=L/2 has increases significantly as seen in figure 11, and it reacts to the air temperature change more than the previous case and vice versa.

As we can see in figure 12, for low thermal conductivity, it took a longer time to change the temperature of the ground up to a significant extent at x=L/2. This is because the heat can not propagate quickly when the value of the thermal conductivity is small. Thus, our case follows this physical phenomenon.

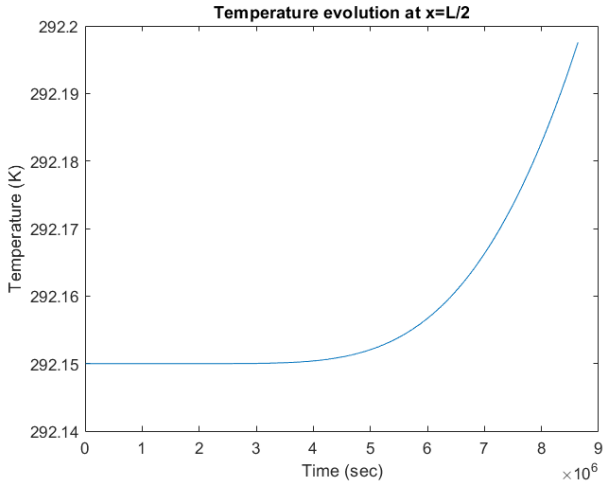

Figure 10: Temperature evolution at x=L/2 for $\lambda=1.6\times10^{-2}$ W/mK.

Similarly, we checked the physical property of specific heat for our case as well. In the reference case, the value of the specific heat was 700 J/kgK. Since it is a large value of specific heat, it takes a while for the temperature of the ground to change its temperature, as it requires large amount of energy to change 1K of temperature difference. To check this, we reduced the value of the specific heat from 700 J/kgK to 7 J/kgK. We noticed that the temperature change requires less energy, thus the temporal variation is more significant at x=L/2, as seen in figure 13.

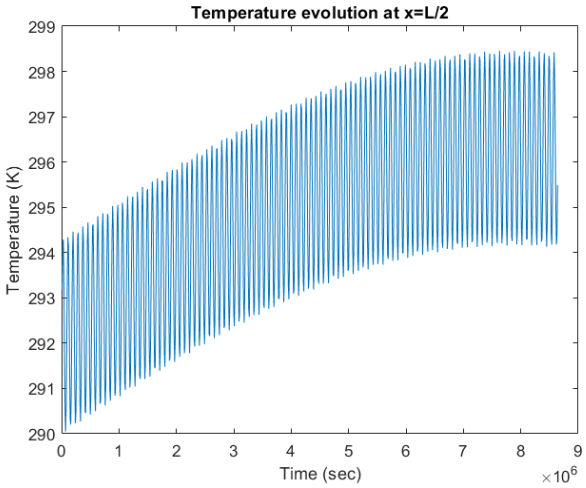

Figure 11: Temperature evolution at x=L/2 for C_p=7 J/kgK.

To check the opposite phenomenon, we increased the value of thermal conductivity to 70000 J/kgK. This value signifies that it would take 70000 J equivalent amount of energy to increase 1K temperature of 1kg material. This is evident in figure 14, as it can be seen that for a large period of time, the temperature of the ground does not change at x=L/2, because with this value of specific heat, the ground acts more like a heat storage, where it stores more energy with very little temperature increase.

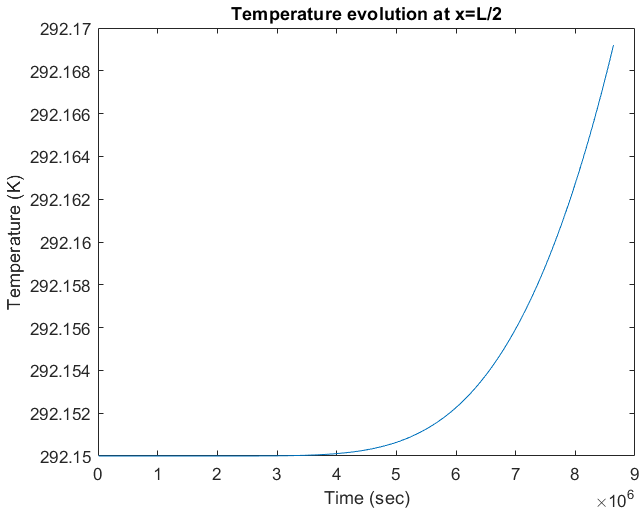

Figure 12: Temperature evolution at x=L/2 for C_p=70000 J/kgK.

Conclusion:

Since the ground in our reference case, has higher value of specific heat and density while having lower value of thermal conductivity, it acted more like a heat sink where temperature does not change significantly with absorbed temperature. The whole problem signifies how the change in adjacent air temperature causes a heat flux between the ground and the environment. We could see from the illustrations that the heat flux propagates through the ground, while slowly getting damped because of the thermophysical properties of the ground. Our code was able to follow the real case phenomenon and physical laws properly, which was verified using energy balance and several parametric studies.